

Article

Sewage Sludge Bio-Oil Development and Characterization

Zeban Shah ¹, Renato Cataluña Veses ¹, Jonatan Brum ¹, Marcos Antônio Klunk ², Luiz Alberto Oliveira Rocha ^{2,*}, André Brum Missaggia ³, Andressa Padilha de Oliveira ³ and Nattan Roberto Caetano ³

¹ Federal University of Rio Grande do Sul, Av. Bento Gonçalves 9500, 91501-970 Porto Alegre, RS, Brazil; zeban.shah@ufrgs.br (Z.S.); rcv@ufrgs.br (R.C.V.); j.brum@ufrgs.br (J.B.)

² University of Vale do Rio dos Sinos, Av. Unisinos 950, 93020-190 São Leopoldo, RS, Brazil; marcosak@edu.unisinos.br

³ Federal University of Santa Maria, Av. Roraima 1000, 97105-900 Santa Maria, RS, Brazil; andremissaggia@hotmail.com (A.B.M.); padilha_andressa@hotmail.com (A.P.d.O.); nattan.caetano@ufsm.br (N.R.C.)

* Correspondence: luizor@unisinos.br

Received: 21 May 2020; Accepted: 27 July 2020; Published: 29 July 2020



Abstract: This work presents the production of sewage sludge oil by pyrolysis, shows the physicochemical properties and compares it with commercial diesel. The sewage sludge was dried and mixed to discarded cooking oil to increase the fuel conversion rate due to the pyrolysis process at an initial temperature of 25 °C and a final of 650 °C. The oil was distilled and analyzed in a Proton nuclear magnetic resonance (1H-NMR), Gas Chromatogram and Mass spectrometry (GC-MS), thermogravimetric analysis (TGA) and Fourier transform infrared spectroscopy (FTIR) to perform a structural characterization on the molecular distribution, groups of functions and the product thermal stability. The authors measured fundamental physicochemical properties like viscosity, density and flashpoint and compared the results with the corresponding commercial S-10 diesel properties observing good agreement.

Keywords: pyrolysis; physicochemical properties; S-10 diesel

1. Introduction

Sewage Sludge is the residual product from the treatment of sewage of industrial and municipal wastewater. Sewage sludge is an environmental question in terms of human health [1–3]. The amount of sludge is increasing in the last years, which can cause a risk to the environment and health [1,2,4,5]. Pathogens remain in sewage sludge without treatment. However, it is safe when appropriately treated [3,6,7]. Some reversible treatments can overcome problems in sewage sludge [8,9]. Pyrolysis is one alternative to convert several residues and biomasses to extract important chemical and bio-oil [8–12].

Organic solid wastes materials are renewable energy sources [13,14], which are processed, applying several different methods to produce energy [15–17]. Since the thermochemical processes, pyrolysis has mainly been used due to optimize the process conditions to increase oil production. The product obtained from wastes by pyrolysis is a raw fuel, perhaps it can be post-processed to generate refined fuel [18–20].

The focus of several works was on the production of liquids by the pyrolysis of organic wastes. The specific case of sewage sludge is to be employed as a fertilizer of soil for crops growing among many purposes of the pyrolysis [21–24].

The sewage sludge production depends on the wastewater treated concentration, which also depends on the class of process of treatment of the wastewater, which can be measured in kg for dry solids per wastewater treated cubic meter [25–28]. Sludge was spread to land as an amendment for soil and for growing crops fertilizer directly due to contains nitrogen-containing compounds [29–33].

The main concern of the treated sludge is the content of the metals (cadmium, copper, arsenic, as is, which are micronutrients for plants) because these metals are regulated. Leaching methods are suitably applied to reduce the content and satisfy the limits on the level of metals, chemicals and others observed in sewage sludge samples [34–40].

This work used a reactor to provide the recovery oil in sewage sludge and the sewage sludge joint with discarded cooking oil, from 25 to 650 °C and residence time from 45 to 65 min. thermogravimetric analysis (TGA) and Gas Chromatogram and Mass spectrometry (GC-MS) were employed to determine the molecular distribution, thermal stability and structure of sewage sludge pyrolysis oil.

2. Experimental

2.1. Materials

The experimental work consisted of drying sewage sludge collected from drainage using an electric oven for 12 h. A restaurant provided discarded oil from cooking. The diesel oil used in this work was the S-10 type commercialized in Brazil.

2.2. Production

The SSP was generated without the use of catalysts. The sample weight was kept 300 g of the sewage sludge sample during the pyrolysis. A reactor of stainless steel was used for the pyrolysis system, shown in Figure 1. The reactor temperature began at 25 °C and was increased to 650 °C through a temperature controller. The sample of sewage sludge was converted into oil and captured by condensers. These fractions were taken and characterized.



Figure 1. Pyrolysis system: (A) Heat or temperature controller; (B) Pressure maintainer; (C) Main electric furnace (biomass); (D) Condenser with 100 °C; (E) Condenser with 5 °C; (F) Cooler; (G) Hot water pump.

2.3. GC-MS

The compositions determination of SSP was performed using an Agilent GC model 6890, with a mass controller Agilent, model 5973, capillary polar wax column, polyethylene glycol (PEG)-coated (of 30 m length, 0.25 mm internal diameter and 0.25 μm film thickness). Conditions of chromatographic were—Injection volume of 0.2 μL , oven at 40 $^{\circ}\text{C}$ (1 min) 6 $^{\circ}\text{C min}^{-1}$ up to 300 $^{\circ}\text{C}$ (10 min^{-1}) split mode at 100:1 ratio and 280 $^{\circ}\text{C}$ of the temperature of injection. Time-released of 55 min and Helium was used as a carrier gas in 2.9 mL min^{-1} of flow rate.

2.4. ($^1\text{H-NMR}$)

The spectra of Proton nuclear magnetic resonance, $^1\text{H-NMR}$, were captured using a spectrometer Varian, model VRMN-300 MHz. Also, the analysis of nuclear magnetic resonance was operated using chloroform (deuterated).

2.5. Thermogravimetric Analysis

The SSP analysis, in terms of thermogravimetric, was made to measure the sample thermal properties. In this case, a pure nitrogen gas, in a flow rate of 100 mL min^{-1} , was purged to fluid displace in the pyrolysis region to avoid sample oxidation. Also, an alumina crucible was employed in a TA Instruments model SDT Q600.

2.6. Fourier Transform Infrared

The Fourier transform infrared detected different organic chemical functional groups present in sewage sludge pyrolysis oil. The infrared spectrums were achieved in a wafer film form on potassium bromide (KBr), applying the FTIR spectrophotometer (Varian 2000 FTIR) in 4000–400 cm^{-1} of the frequency range.

2.7. Enthalpy of Combustion

The calorimeter, VEB Vereinigte Babelsberger App-Nr., Model 081036, was employed to calculate the calorific value, that is, the calorific value measuring the variation of the temperature achieved from produced heat transferred due to the combustion. Thus, the SSP analysis was made in a calorimeter at adiabatic conditions.

2.8. Flashpoint

The simple open cup method was applied to determine the flashpoints of SSP, using a thermometer, a heater and a gas flame.

2.9. Density, Viscosity and pH

A 250 mm Cannon-Fenske viscometer was applied to measure the SSP viscosity and also to S-10 Diesel at six different temperatures, from -10 to 50 $^{\circ}\text{C}$ and a simple g.mL^{-1} method to verify the density under the same temperatures. The pH of the sample was measured by proof of Eutechwater (pH Spear 510).

3. Results and Discussions

3.1. Influence of Temperature on Pyrolysis Yield

Several pyrolysis measurements were performed to determine the temperature, which maximizes the fuel oil yielding from sewage sludge. This oil produced, water, gases and biochar of 30 mm diameter and temperature between 450 to 650 $^{\circ}\text{C}$ at 20 $^{\circ}\text{C min}^{-1}$, as shown in Table 1.

Note that the liquid phase product presented a clear increase in rising temperatures from 450 $^{\circ}\text{C}$ to 650 $^{\circ}\text{C}$. Similar behaviors were also observed in the literature [23,36]. The gas non-condensable

was observed as increased from 9% to 13% at a higher temperature. Table 1 shows that the oil yield increased proportionally to temperature and at 650 °C, the maximum yield was achieved, that is, 13%. Thus, it was observed that the pyrolysis oil quantity yielded depends on the temperature in the reactor and biomass class [9].

Table 1. Changes in the pyrolysis yields at different pyrolysis temperatures.

No.	Sample (In Grams)	T (°C)	Liquid-Oil (% Weight)	Uncondensablegas (% Weight)	Residues (%Weight)	Water Fraction (% Weight)
1	300	450	7	9	72	10
2	300	550	8	13	69	10
3	300	650	13	13	66	10

3.2. GC-MS

Mainly 34 organic compounds were found in SSP, as shown in Table 2 and these compounds can be classified in higher classes as oxygenates, hydrocarbons, alcohols, phenols and nitrogenizes as shown in the literature [6,15,17,33]. The oil sample was analyzed using GC-MS (Figure 2) and 15% of hydrocarbons were identified.

Table 2. Compounds identified in SSP.

No.	Compound's Names	Formulas	Retention Time	Percent Area
1	Phenol	C ₆ H ₆ O	09.01	2.77
2	Phenol, 2-methyl-	C ₇ H ₈ O	10.02	1.34
3	Phenol, 3-methyl-	C ₇ H ₈ O	11.04	1.10
4	Phenol, 2,5-dimethyl-	C ₈ H ₁₀ O	12.02	1.69
5	Azulene	C ₁₀ H ₈	14.00	1.30
6	Naphthalene, 2-methyl	C ₁₁ H ₁₀	15.02	1.40
7	Naphthalene, 1-methyl-	C ₁₁ H ₁₀	16.10	1.29
8	3-Heptadecene	C ₁₇ H ₃₄	18.11	1.60
9	1-Pentadecene	C ₁₅ H ₃₀	20.01	1.50
10	Hexadecane	C ₁₈ H ₃₈	21.10	1.31
11	1-Heptadecene	C ₁₇ H ₃₄	23.11	1.36
12	Tricosane	C ₂₃ H ₄₈	24.00	0.95
13	Hexadecanenitrile	C ₁₆ H ₃₁ N	25.21	2.20
14	Methylhexadecanoate	C ₁₇ H ₃₄ O ₂	27.20	4.50
15	Hexadecanoicacid	C ₁₆ H ₃₂ O ₂	29.22	5.10
16	Hexadecanoic acid, ethyl ester	C ₁₈ H ₃₆ O ₂	30.10	3.75
17	Triolein	C ₅₇ H ₁₀₄ O ₆	31.00	4.50
18	Ethylpentadecanoate	C ₁₇ H ₃₄ O ₂	33.22	2.90
19	Ethanone	C ₈ H ₁₂ O	34.23	4.90
20	Cyclohexene,3-(2-propenyl)-	C ₉ H ₁₄	35.01	1.20
21	Benzene, 1,3,5-trimethyl-	C ₉ H ₁₂	36.38	0.75
22	Decane	C ₁₀ H ₂₂	37.22	1.15
23	Cyclohexene,3-(2-propenyl)-	C ₉ H ₁₄	38.34	1.19
24	Toluene	C ₇ H ₇	39.12	2.31
25	Pyridine	C ₅ H ₅ N	40.33	2.55
26	Octadecenamamide	C ₁₈ H ₃₅ NO	42.11	2.35
27	1H-pyrrole	C ₄ H ₅ N	43.33	2.45
28	p-Cresol	C ₇ H ₈ O	44.01	3.44
29	Benzofuran	C ₈ H ₆ O	45.33	2.98
30	Chrysene	C ₁₈ H ₁₂	46.11	2.34
31	Furfuryl	C ₅ H ₆ O ₂	47.11	3.30
32	Isoquinoline	C ₉ H ₇ N	47.54	2.55
33	Octadecenoicacid, methylester	C ₁₉ H ₃₆ O ₂	48.01	3.09
34	Ethyl Oleate	C ₂₀ H ₃₈ O ₂	48.50	3.78

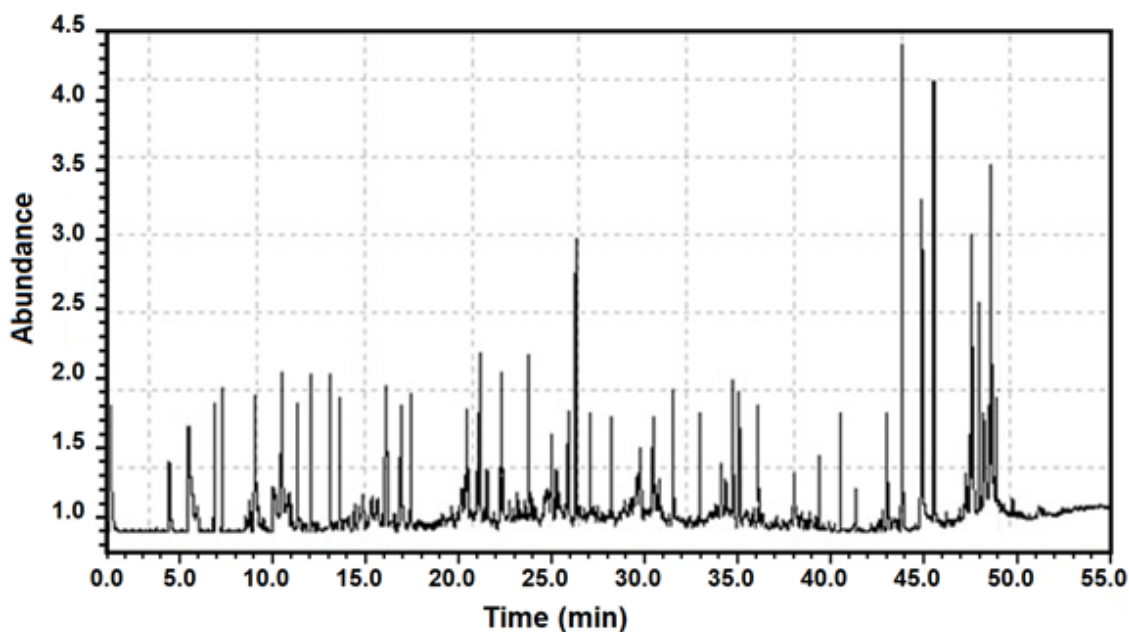


Figure 2. Gas Chromatogram and Mass spectrometry (GC-MS) chromatogram of SSP.

In Table 3, the SSP composition was grouped in chemical classes—alcohol, oxygen-containing compounds, hydrocarbon, phenols and nitrogen compounds (Figure 3). Hydrocarbons (15%) and oxygen compounds (54%) gave the sample class predominance.

Table 3. Different groups of compounds identified in SSP.

No.	Compound's Names	Percent Area	No.	Compound's Names	Percent Area
1	Oxygen containing compounds	54.12	4	N-compounds	13.10
2	Alcohols	6.20	5	Esters	0
3	Phenolic	7.21	6	Hydrocarbons	15.02

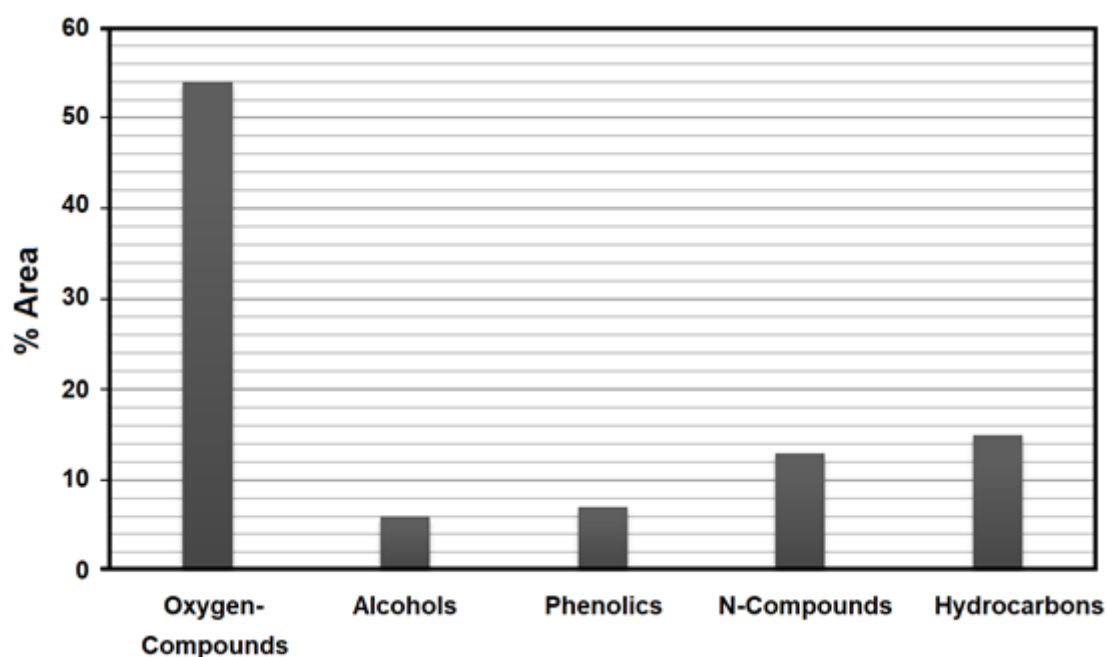


Figure 3. Percent area of all groups identified in SSP.

The SSP was composed mainly of ketones and hydrocarbons, with a low quantity of alcohols, phenols and ethers. The main compounds in the oil are acid (Tetradecanoic acid, Hexadecanoic acid, Octadecenoic acid, etc.). These acids combined have a relative composition of 36%. Moreover, the Hexadecanoic acids were used as cosmetics agents and as coatings oil [19,37].

The hydrocarbons verified in the SSP were classified by groups—n-alkanes and 1-alkenes with several carbons, ranging from C_{11} to C_{31} ; monoaromatic hydrocarbons including toluene, benzene, styrene, 1H-indene and the alkyl derivatives; aromatic compounds, containing nitrogen and oxygen as pyridine, alkyl pyridines, isoquinoline, 1H-pyrrole, methylquinolines, 1H-indole, 9H-carbazole and benzofurane; aromatic nitriles and aliphatic; carboxylic acids, in which R represents long aliphatic chains of 13, 14, 15 and 17 carbons; long-chain aliphatic amides and steroids as cholestene, formyl cholestene or cholestadiene [10,14,25].

3.3. 1H NMR

Figure 4 presents aromatic hydrogens, verified by signals in the region of 5 to 7 ppm, as hydrogens bound to oxygenated carbons (CH–O) from 2.0 to 3.0 ppm and of hydrogens near of carbonyl in the region between 1.0 and 2.0 ppm. The intense peaks appear at 0.7 and 1.5 as typical of aliphatic hydrogens.

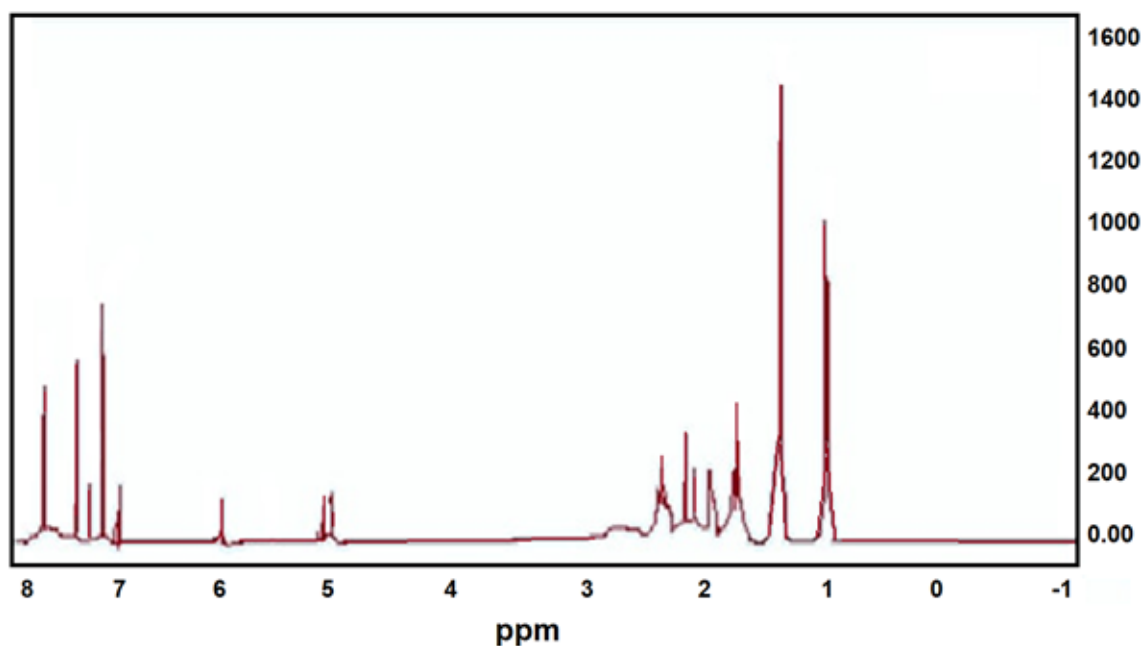


Figure 4. 1H NMR spectrums of SSP.

The hydrogen percentage distribution was measured based on chemical shift values from the 1H -NMR spectra. The aromatic proton observed in the chemical shift region between 6.0–8.0 ppm and the amount of maximum proton attached to β - CH_3 , CH_2 and CH_γ to an aromatic ring accounted for in the chemical shift region of 1.5–1.0 ppm, although olefinic proton was found in the region between 5–5.7 ppm [38,39]. The proton attached to CH_3CH_2 and CH to an aromatic ring lay in the chemical shift range of 2.0–3.0 ppm.

3.4. TGA

Figure 5 shows the sample's thermogram, in which the majority of the mass (98.49%) was decomposed at 200 °C. Thermogram also shows a material that was not undergoing decomposition from 300 to 450 °C, which is due to high molecular weight organic substances [9,14,19], which generates wastes of 1.50%, due after pyrolysis [35]. That is the reason of this 1.50% of waste.

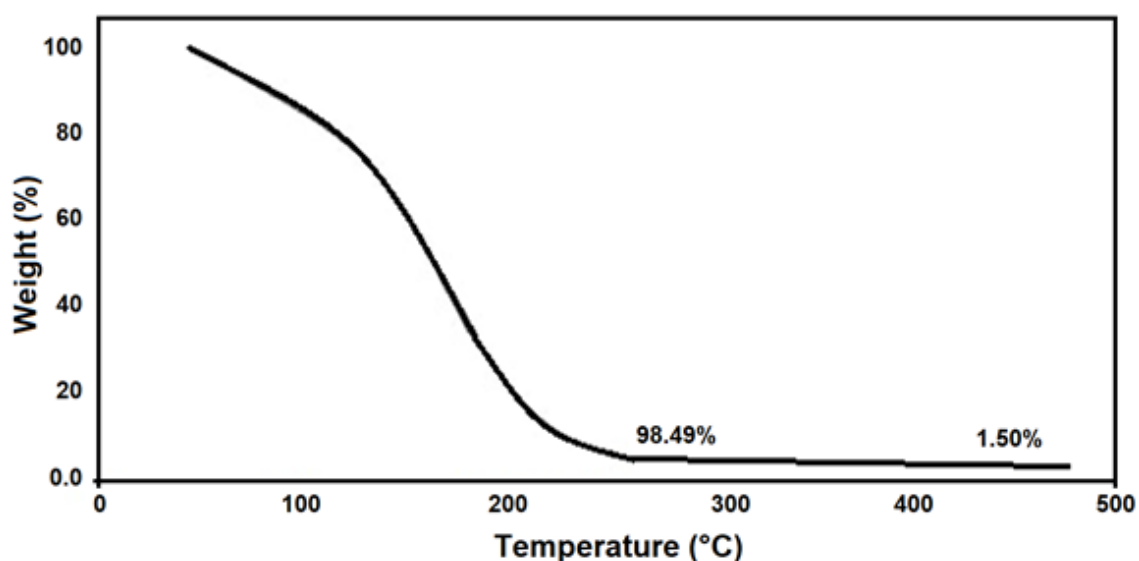


Figure 5. TGA thermogram of SSP.

Figure 5 also shows the lowest quantity of residue contents, which contributes to the fraction of fuel mixture with diesel. The waste produced after the process shows a lower value due to the absence of highly reactive organic compounds [40].

3.5. FTIR Analysis

Figure 6 shows the FTIR spectrum, which provides several functional groups present in the SSP. The spectrum shows the absorption bands at 2955, 2855, 1713, 1522, 1377, 1026 and 756 cm^{-1} , which are characteristic to different functional groups identified in SSP. The absorption bands at around 3000 cm^{-1} are due to the symmetric and asymmetric vibration of saturated C-H bonds [7,19], while the absorption band at 1457 cm^{-1} is associated with the asymmetric deformation of the CH methyl and methoxyl groups. The broadened band at 2963.98 cm^{-1} is the stretching vibration of the OH bond characteristic [10,14,35]. The band at 1713.42 cm^{-1} is related to the C=O stretching vibration.

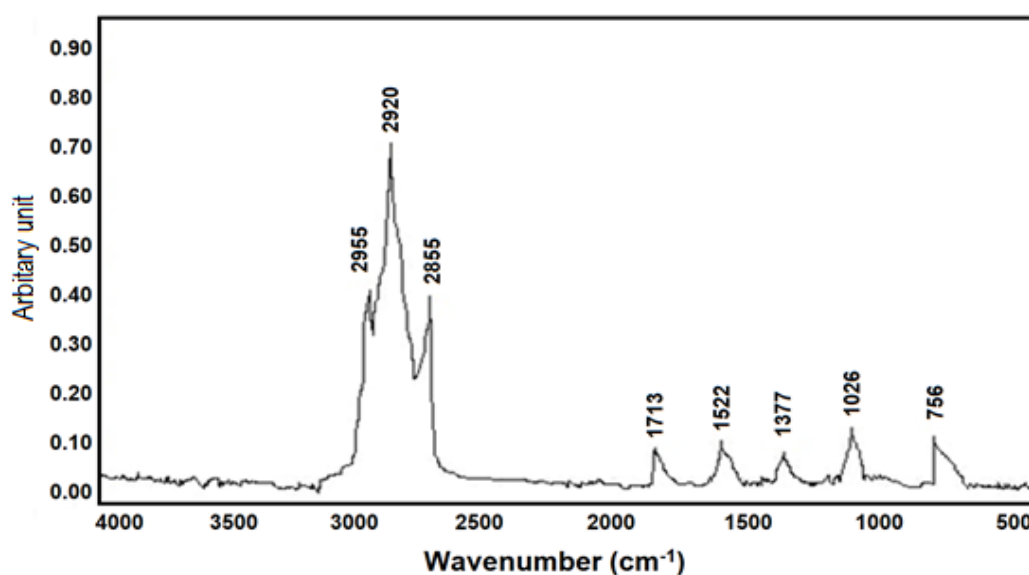


Figure 6. Fourier transform infrared (FTIR) spectra of functional groups identified in SSP.

3.6. Calorific Value

A calorimeter was applied to measure the enthalpy of combustion for SSP and diesel. Table 4 shows the value of SSP, 39.16 MJ kg⁻¹ and 43.40 MJ kg⁻¹ for diesel.

Table 4. Calorific value, flash point, density and viscosity SSP and S-10 Diesel.

Fractions	SSP	S-10 Diesel
Calorific Value (MJ kg ⁻¹)	39.16	43.40
Flash point (°C)	70.00	63.00
Density (g mL ⁻¹) at 25 °C	0.8231	0.8354
Viscosity (mm ² s ⁻¹) at 25 °C	1.6274	1.8484

3.7. Density and Viscosity

Tables 5 and 6 present the changes at several temperatures in SSP density and viscosity and S-10 diesel. The SSP density and viscosity were observed as similar to S-10. It was noticed that the SSP viscosity was 1.7% higher than S-10 and a difference of 2% between the SSP densities and diesel were observed.

Table 5. Density of SSP at different temperatures.

T (K)	T (°C)	Volume (mL)	Mass (g)	ρ (g mL ⁻¹) S-10 Diesel	ρ (g mL ⁻¹) SSP
283	10	11.955	10	0.8398	0.8364
293	20	11.999	10	0.8367	0.8334
303	30	12.141	10	0.8311	0.8236
313	40	12.211	10	0.8256	0.8189
323	50	12.294	10	0.8223	0.8134

Table 6. Viscosity of SSP at different temperatures.

T(°C)	Flow Time (s)	T (K)	η (mm ² /s) S-10 Diesel	η (mm ² /s) SSP
10	210	283	1.7625	1.6531
20	180	293	1.2131	0.9673
30	172	303	0.8827	0.8523
40	150	313	0.8343	0.8273
50	142	323	0.7434	0.7223

3.8. Flash Points and pH

The SSP flashpoint was obtained at 70 °C and S-10 Diesel at 63 °C. The SSP's pH was measured as 5.1, as seen in other bio-oils, which are usually acidic and contain distinct quantities of organic acids [20].

3.9. Chemical Composition

The SSP appearance was observed as a dark brown liquid. The compounds detected were classified into hydrocarbons, alcohols, phenol, oxygen and nitrogen compounds. Also, wide peaks of GC-MS show in majority oxygen-containing compounds and hydrocarbons. The main part of SSP contained oxygen-containing compounds, while alcohols, phenols and nitrogenated compounds can be seen in SSP as presented in Figure 3 and Table 2.

4. Conclusions

Sewage sludge oil was produced from a collected drainage line in which some treatments to convert into pyrolysis oil were performed. In this product, only 3% was found as fuel. Thus, discarded cooking oil was added to increase the yielding of the product. In this way, it was observed that the fuel yield increases by up to 13%.

The oil from the pyrolysis of sewage sludge was found as a complex liquid and the compounds verified in sludge oil were oxygen-containing and a few concentration of hydrocarbons and alcohols.

The physic-chemical properties of sewage sludge oil were compared with S-10 diesel and the results were found as similar.

The waste of sewage sludge after pyrolysis is useful for several purposes as crop fertilizers. These products, like the fertilizers or the processing costs, are high. However, it may be attractive as environment protection.

Author Contributions: Conceptualization, Z.S.; Data curation, R.C.V., M.A.K. and N.R.C.; Formal analysis, R.C.V., M.A.K., A.P.d.O., N.R.C. and L.A.O.R.; Investigation, R.C.V., J.B., A.B.M., A.P.d.O., N.R.C. and L.A.O.R.; Methodology, Z.S., A.B.M., A.P.d.O. and N.R.C.; Visualization, M.A.K.; Writing—original draft, Z.S.; Writing—review & editing, L.A.O.R. All authors have read and agreed to the published version of the manuscript.

Funding: This research received no external funding.

Acknowledgments: This work was supported by CNPq, Brasília, DF, Brazil.

Conflicts of Interest: The authors declare no conflict of interest.

References

1. Wei, F.; Cao, J.-P.; Zhao, X.-Y.; Ren, J.; Gu, B.; Wei, X.-Y. Formation of aromatics and removal of nitrogen in catalytic fast pyrolysis of sewage sludge: A study of sewage sludge and model amino acids. *Fuel* **2018**, *218*, 148–154. [[CrossRef](#)]
2. Veses, R.C.; Shah, Z.; Pelisson, L.; Caetano, N.R.; Silva, R.D.; Azevedo, C.M.N. Biodiesel Glycerides from the Soybean Ethylic Route Incomplete Conversion on the Diesel Engines Combustion Process. *J. Braz. Chem. Soc.* **2017**, *28*, 2447–2454. [[CrossRef](#)]
3. Gomaa, M.A.; Gombocz, N.; Schild, D.; Mjalli, F.S.; Al-Harrasi, A.; Abed, R.M.M. Effect of organic solvents and acidic catalysts on biodiesel yields from primary sewage sludge, and characterization of fuel properties. *Biofuels* **2018**, 1–9. [[CrossRef](#)]
4. Areeprasert, C.; Chanyavanich, P.; Ma, D.; Shen, Y.; Yoshikawa, K. Effect of hydrothermal treatment on co-combustion of paper sludge with coal: Thermal behavior, NO emissions, and slagging/fouling tendency. *Biofuels* **2016**, *8*, 187–196. [[CrossRef](#)]
5. Antony, D.; Murugavelh, S. Anaerobic co-digestion of kitchen waste and wastewater sludge: Biogas-based power generation. *Biofuels* **2016**, *9*, 157–162. [[CrossRef](#)]
6. Sanchez, M.E.; Menendez, J.A.; Dominguez, A.; Pis, J.J.; Martinez, O.; Calvo, L.F.; Bernad, P.L. Effect of pyrolysis temperature on the composition of the oils obtained from sewage sludge. *Biomass Bioenergy* **2009**, *33*, 933–940. [[CrossRef](#)]
7. Werther, J.; Ojada, T. Sewage sludge combustion. *Prog. Energy Combust. Sci.* **1999**, *25*, 55–116. [[CrossRef](#)]
8. Piskorz, J.; Scott, D.S.; Westerberg, I.B. Flash pyrolysis of sewage sludge. *Ind. Eng. Chem. Process Des. Dev.* **1986**, *25*, 265–270. [[CrossRef](#)]
9. Domínguez, A.; Menéndez, J.A.; Inguanzo, M.; Pis, J.J. Gas chromatographic-mass spectrometric study of the oil fractions produced by microwave-assisted pyrolysis of different sewage sludges. *J. Chromatogr. A* **2003**, *1012*, 193–206. [[CrossRef](#)]
10. Shah, Z.; Veses, R.C.; Vagheti, J.C.P.; Amorim, V.D.A.; da Silva, R. Preparation of jet engine range fuel from biomass pyrolysis oil through hydrogenation and its comparison with aviation querosene. *Int. J. Green Energy* **2019**, 1–11. [[CrossRef](#)]
11. Lu, G.Q.; Flow, J.C.; Lin, C.Y.; Lua, A.C. Surface area development of sewage sludge during pyrolysis. *Fuel* **1995**, *74*, 344–348. [[CrossRef](#)]

12. Zakaria, R.; Harvey, A.P. Direct production of biodiesel from rapeseed by reactive extraction/in situ transesterification. *Fuel Process. Technol.* **2012**, *102*, 53–60. [[CrossRef](#)]
13. Vassilev, S.V.; Baxter, D.; Andersen, L.K.; Vassileva, C.G.; Morgan, T.J. An overview of the organic and inorganic phase composition of biomass. *Fuel* **2012**, *94*, 1–33. [[CrossRef](#)]
14. Shah, Z.; Renato, C.V.; Marco, A.C.; Rosangela, D.S. Separation of Phenol from Bio-oil Produced from Pyrolysis of Agricultural Wastes. *Mod. Chem. Appl.* **2017**, *5*, 1–8. [[CrossRef](#)]
15. Wu, Q.; Zhang, B.; Grant, N.G. High yield of hydrocarbon gases resulting from pyrolysis of yellow heterotrophic and bacterially degraded *Chlorella protothecoides*. *J. Appl. Phycol.* **1996**, *8*, 181–184. [[CrossRef](#)]
16. Du, J.; Liu, P.; Liu, Z.; Sun, D.; Tao, C. Fast pyrolysis of biomass for bio-oil with ionic liquid and microwave irradiation. *J. Fuel Chem. Technol.* **2010**, *38*, 554–559. [[CrossRef](#)]
17. Ji, Y.; Hou, Y.; Ren, S.; Yao, C.; Wu, W. Separation of phenolic compounds from oil mixtures using environmentally benign biological reagents based on Brønsted acid-Lewis base interaction. *Fuel* **2019**, *239*, 926–934. [[CrossRef](#)]
18. Shah, Z.; Veses, R.C.; Silva, R.D. GC-MS and FTIR analysis of bio-oil obtained from freshwater algae (*spirogyra*) collected from Freshwater. *Int. J. Environ. Agric. Res.* **2016**, *2*, 134–141.
19. Zhan, H.; Yin, X.; Huang, Y.; Zhang, X.; Yuan, H.; Xie, J.; Wu, C. Characteristics of NO_x precursors and their formation mechanism during pyrolysis of herb residues. *J. Fuel Chem. Technol.* **2017**, *45*, 279–288. [[CrossRef](#)]
20. Caetano, N.R.; Venturini, M.S.; Centeno, F.R.; Lemmert, C.K.; Kyprianidis, K.G. Assessment of mathematical models for prediction of thermal radiation heat loss from laminar and turbulent jet non-premixed flames. *Therm. Sci. Eng. Prog.* **2018**, *7*, 241–247. [[CrossRef](#)]
21. Wander, P.R.; Bianchi, F.M.; Caetano, N.R.; Klunk, M.A.; Indrusiak, M.L.S. Cofiring low-rank coal and biomass in a bubbling fluidized bed with varying excess air ratio and fluidization velocity. *Energy* **2020**, *203*, 117882. [[CrossRef](#)]
22. Rahman, M.M.; Liu, R.; Cai, J. Catalytic fast pyrolysis of biomass over zeolites for high quality bio-oil—A review. *Fuel Process. Technol.* **2018**, *180*, 32–46. [[CrossRef](#)]
23. Chen, T.; Wu, J.; Zhang, Z.; Zhu, M.; Sun, L.; Wu, J.; Zhang, D. Key thermal events during pyrolysis and CO₂-gasification of selected combustible solid wastes in a thermogravimetric analyser. *Fuel* **2014**, *137*, 77–84. [[CrossRef](#)]
24. Shah, Z.; Veses, R.C.; Silva, R.D. Using GC-MS to Analyze Bio-Oil Produced from Pyrolysis of Agricultural Wastes—Discarded Soybean Frying Oil, Coffee and Eucalyptus Sawdust in the Presence of 5% Hydrogen and Argon. *J. Anal. Bioanal. Tech.* **2016**, *7*, 1–7. [[CrossRef](#)]
25. Li, H.; Yan, Y.; Ren, Z. Online upgrading of organic vapors from the fast pyrolysis of biomass. *J. Fuel Chem. Technol.* **2008**, *36*, 666–671. [[CrossRef](#)]
26. Vaish, B.; Sharma, B.; Srivastava, V.; Singh, P.; Ibrahim, M.H.; Singh, R.P. Energy recovery potential and environmental impact of gasification for municipal solid waste. *Biofuels* **2017**, 1–14. [[CrossRef](#)]
27. Oyebanji, J.A.; Okekunle, P.O.; Lasode, A.O.; Oyedepo, S.O. Chemical composition of bio-oils produced by fast pyrolysis of two energy biomass. *Biofuels* **2017**, *9*, 479–487. [[CrossRef](#)]
28. Caetano, N.R.; Silva, B.P. Technical and Economic Viability for the Briquettes Manufacture. *Defect Diffus. Forum* **2017**, *380*, 218–226. [[CrossRef](#)]
29. Klunk, M.A.; Dasgupta, S.; Das, M. Influence of Fast Pyrolysis with Temperature on Gas, Char and Bio-oil Production. *South. Braz. J. Chem.* **2017**, *25*, 1–11.
30. Parthasarathy, P.; Gupta, N.K.; Narayanan, K.S. Effect of composting on products of slow pyrolysis. *Biofuels* **2015**, *6*, 313–321. [[CrossRef](#)]
31. Westover, T.L.; Phanphanich, M.; Clark, M.L.; Rowe, S.R.; Egan, S.E.; Zacher, A.H.; Santosa, D. Impact of thermal pretreatment on the fast pyrolysis conversion of southern pine. *Biofuels* **2013**, *4*, 45–61. [[CrossRef](#)]
32. Veses, R.C.; Shah, Z.; Venturi, V.; Caetano, N.R.; da Silva, B.P.; Azevedo, C.M.N.; Da Silva, R.; Suarez, P.A.Z.; Oliveira, L.P. Production process of di-amyl ether and its use as an additive in the formulation of aviation fuels. *Fuel* **2018**, *228*, 226–233. [[CrossRef](#)]
33. Caetano, N.R.; Veses, R.C.; Vielmo, H.A. Analysis of the Effect on the Mechanical Injection Engine Using Doped Diesel Fuel by Ethanol and Bio-Oil. *Int. Rev. Mech. Eng.* **2015**, *9*, 124–128. [[CrossRef](#)]
34. Shah, Z.; Veses, R.C.; Silva, R.D. A Comparative Study and Analysis of Two Types of Bio-Oil Samples Obtained from Freshwater Algae and Microbial Treated Algae. *Mod. Chem. Appl.* **2016**, *4*, 1–7. [[CrossRef](#)]
35. Demirel, Y. Lignin for Sustainable Bioproducts and Biofuels. *J. Biochem. Eng. Bioprocess Technol.* **2017**, *1*, 1–3.

36. Shah, Z.; Veses, R.C.; Aguilhera, R.A.; Silva, R.D. Bio-Oil Production from Pyrolysis of Coffee and Eucalyptus Sawdust in the Presence of 5% Hydrogen. *Int. J. Eng. Res. Sci.* **2016**, *2*, 34–42.
37. Caetano, N.R.; Stapasolla, T.Z.; Peng, F.B.; Schneider, P.S.; Pereira, F.M.; Vielmo, H.A. Diffusion Flame Stability of Low Calorific Fuels. *Defect Diffus. Forum* **2015**, *362*, 29–37. [[CrossRef](#)]
38. Caetano, N.R.; Soares, D.; Nunes, R.P.; Pereira, F.M.; Schneider, P.S.; Vielmo, H.A.; van der Laan, F.T. A comparison of experimental results of soot production in laminar premixed flames. *Open Eng.* **2015**, *5*, 213–219. [[CrossRef](#)]
39. Aboulkas, A.; El Harfi, K.; El Bouadili, A. Pyrolysis of olive residue/low density polyethylene mixture: Part I Thermogravimetric kinetics. *J. Fuel Chem. Technol.* **2008**, *36*, 672–678. [[CrossRef](#)]
40. Yao, C.; Hou, Y.; Ren, S.; Wu, W.; Ji, Y.; Liu, H. Sulfonate based zwitterions: A new class of extractants for separating phenols from oils with high efficiency via forming deep eutectic solvents. *Fuel Process. Technol.* **2018**, *178*, 206–212. [[CrossRef](#)]



© 2020 by the authors. Licensee MDPI, Basel, Switzerland. This article is an open access article distributed under the terms and conditions of the Creative Commons Attribution (CC BY) license (<http://creativecommons.org/licenses/by/4.0/>).